Title: Characterization of a thermostable, specific GH10 xylanase from *Caldicellulosiruptor bescii* with high catalytic activity

Author: Jiao An Yuan Xie Yong Zhang Dongsheng Tian Shuhao Wang Guangyu Yang Yan Feng

PII: S1381-1177(15)00101-0
DOI: http://dx.doi.org/doi:10.1016/j.molcatb.2015.04.003
Reference: MOLCAB 3143

To appear in: *Journal of Molecular Catalysis B: Enzymatic*

Received date: 14-10-2014
Revised date: 17-3-2015
Accepted date: 4-4-2015

Please cite this article as: J. An, Y. Xie, Y. Zhang, D. Tian, S. Wang, G. Yang, Y. Feng, Characterization of a thermostable, specific GH10 xylanase from *Caldicellulosiruptor bescii* with high catalytic activity, *Journal of Molecular Catalysis B: Enzymatic* (2015), http://dx.doi.org/10.1016/j.molcatb.2015.04.003

Characterization of a thermostable, specific GH10 xylanase from *Caldicellulosiruptor bescii* with high catalytic activity

Jiao An [1,2], Yuan Xie[1], Yong Zhang[1], Dongsheng Tian[1], Shuhao Wang[1], Guangyu Yang[1*], Yan Feng[1, 2*]

[1] State Key Laboratory of Microbial Metabolism, School of Life Sciences and Biotechnology, Shanghai Jiao Tong University, Shanghai 200240, P.R. China

[2] Key Laboratory for Molecular Enzymology and Engineering of Ministry of Education, Jilin University, Changchun 130021, P.R. China

[*]Corresponding author

To whom correspondence should be addressed:

Guangyu Yang, State Key Laboratory of Microbial Metabolism, Shanghai Jiao Tong University, 800 Dongchuan Rd. Shanghai 200240, China, Tel: +86-21-34207248; Fax: +86-21-34207189, E-mail: yanggy@sjtu.edu.cn

Yan Feng, State Key Laboratory of Microbial Metabolism, College of Life Sciences and Biotechnology, Shanghai Jiao Tong University, 800 Dongchuan Road, Shanghai 200240, P. R. China. Tel & Fax: 86-21-34207189, E-mail: yfeng2009@sjtu.edu.cn

Abstract

Xylanase (EC 3.2.1.8) is one of the most important enzymes for the biodegradation of xylan. Since many industrial processes utilizing xylanase are operated at elevated temperatures, thermostable xylanases are highly desirable. In the present study, *xyn10B* gene from thermophilic bacterium *Caldicellulosiruptor bescii* that encodes a glycoside hydrolase (GH) family 10 xylanase was overexpressed in *Escherichia coli* and systematically characterized. CbXyn10B exhibited optimal activity at pH 7.2 and 70 °C. It had a half-life of about 7.7 h at 60 °C, and retained over 85% of maximal activity after incubation at pH 4.0-12.0. The activity of this xylanase was not affected by most divalent cations, but inhibited by Fe^{3+} and Zn^{2+}. CbXyn10B exhibited high activity on beech wood xylan, oat spelt xylan, and birch wood xylan, with specific activities of about 450 U mg^{-1}. Compared with other GH10 xylanases, CbXyn10B

was highly specific for xylan and showed low catalytic efficiency towards sodium carboxymethyl cellulose and *p*-nitrophenyl-β-D-xylopyranoside. HPLC analysis of the products released from xylo-oligosaccharides and xylan revealed that xylobiose was the predominant hydrolytic product. The action mode of the enzyme was studied by product analysis, homology modeling and molecular docking to gain an insight into the structural basis for its substrate recognition mechanism.

Keywords

GH10 xylanase; *Caldicellulosiruptor bescii*; Substrate specificity; Thermostability; Xylans; Xylooligosaccharides.

1. Introduction

Xylan, as the major constituent of plant cell walls, is the second most abundant polysaccharide in nature and accounts for approximately one-third of all renewable organic carbon on earth [1]. Biodegradation of xylan requires the coordinate action of several enzymes, such as endo-β-1,4-xylanase (xylanase for short), β-D-xylosidase, α-L-arabinofuranosidase, α-D-glucuronidase, acetylxylan esterase and feruloyl esterases [2]. Among these, xylanases (EC 3.2.1.8) that cleave internal linkages on the β-1,4-xylose backbone play a leading role. Xylanases are produced by many microorganisms, including bacteria, actinomycetes, protozoa and fungi [3, 4]. These enzymes vary in primary sequences, structure folds, substrate specificities and catalytic mechanism [5, 6]. They have been mainly classified into glycoside hydrolase (GH) families 5, 7, 8, 10, 11 and 43 [7]. GH10 xylanases, as one of the most well studied family, typically also have considerable activity towards glucose-derived substrates such as aryl-cello-oligosaccharides [8-10].

Xylanases have immense potential in various biotechnological industries, including the food, feed, textile, waste treatment, bioethanol production and pulp bleaching [11]. However, most known xylanases show maximal activity at temperatures between 40 °C and 60 °C [12], whereas industrial processes favor higher temperatures. In addition, thermostable xylanases that function at elevated temperatures lower the likelihood of microbial contamination, increase reaction rates and substrate solubility and simplify the downstream protein purification [13]. Thus,

the requirement for thermostable xylanases is progressively increased.

Caldicellulosiruptor bescii DSM 6725 is an anaerobic thermophilic bacterium that can efficiently utilize various types of untreated plant biomass. This strain can grow at temperatures as high as 90 °C, which makes it the most thermophilic cellulose-degrading organism known to date [14]. Based on its genome information, *C. bescii* DSM 6725 produces three types of xylanases, including two GH10 xylanases (CbXyn10A and CbXyn10B) and a GH11 xylanase [15]. CbXyn10A is composed of an N-terminal signal-peptide, two carbohydrate-binding domains and a C-terminal catalytic domain, while CbXyn10B possesses only a catalytic domain. It has recently been reported that these two GH10 xylanases are highly thermostable and could work synergistically with other xylan-degrading enzymes from *C. bescii* to hydrolyzed xylan at 65 to 80 °C [16]. To enable CbXyn10B to function under well-defined conditions, a fine characterization of CbXyn10B appears to be desirable.

Here, the gene encoding CbXyn10B was overexpressed in *Escherichia coli*, and recombinant enzyme was purified and further characterized. The mode of action of the enzyme on xylo-oligosaccharides (XOS) was analyzed in detail. In addition, homology modeling and molecular docking were performed to further dissect the structural basis for CbXyn10B action manner.

2. Materials and methods

2.1. Chemicals, strains and plasmids

Xylose (X1), *p*-nitrophenyl-β-xylopyranoside (*p*NPX), *p*-nitrophenyl-β-glucopyranoside (*p*NPG), beech wood xylan, birch wood xylan and oat spelt xylan were purchased from Sigma-Aldrich (St. Louis, USA). Beta-1,4-D-xylooligosaccharides from xylobiose to xylohexaose (X2-X6) were obtained from Megazyme International Ireland Ltd. The pET-28a vector was purchased from Novagen (Darmstadt, Germany). *E. coli* TOP10 and *E. coli* BL21-CodonPlus (DE3)-RIL strains were purchased from Invitrogen (Carlsbad, CA, USA) and they were used for DNA manipulation and recombinant protein production, respectively. *Caldicellulosiruptor bescii* DSM 6725 was obtained from Deutsche Sammlung von Mikroorganismen und Zellkulturen GmbH (DSMZ).

2.2. Multiple sequence alignment and phylogenetic analysis

Homology search was performed with BLAST program at the NCBI web server (http://www.ncbi.nlm.nih.gov/BLAST) [17]. The phylogenetic tree was constructed by Mega 5 software using the neighbor joining method [18]. Sequence alignments were performed with ClustalX [19].

2.3. Cloning and plasmid construction

The *CbXyn10B* gene (GenBank No. ACM59337) was amplified from genomic DNA of *C. bescii* DSM 6725 using the primers *CbXyn10B*_F (5′-CCAGTCCCATGGAGAGCGAAGATTATTATGAAAA-3′) and *CbXyn10B*_R (5′-CGACGACTCGAGAAAGTCAATTATTCTGAAAAATGCC-3′). The PCR products were digested with FD *Nco*I and FD *Xho*I (Fermentas, Shenzhen, China) and inserted into pET-28a expression vector.

2.4. Overexpression and purification of CbXyn10B

The pET28-*CbXyn10B* was expressed in *E. coli* BL21-CodonPlus (DE3)-RIL cells. Cells were grown at 37 °C in 2YT medium supplemented with 100 μg/ml kanamycin until the optical density at 600 nm (OD600) reached 0.6 to 0.8. Gene expression was induced for 16 h at 24 °C by the addition of 1.0 mM isopropyl β-D-1-thiogalactopyranoside (IPTG). The cells were harvested and suspended in 30 mM Tris-HCl buffer (pH 8.0) containing 150 mM NaCl and 30 mM imidazole, and then disrupted by sonication. The cell lysates were heated at 60 °C for 30 min, and the resulting precipitate was removed by centrifugation. The recombinant protein was purified by Ni-NTA affinity chromatography (Qiagen, Hilden, Germany). Protein concentration was measured by the Bradford method with a Bovine Serum Albumin standard set (Fermentas, Shenzhen, China).

2.5. Determination of enzyme activities and properties

The standard assay for xylanase activity was performed at 65 °C in 40 mM pH 7.2 sodium phosphate buffer in the presence of 1.0% (w/v) xylans for 5 min. For CMCase activity, the assay was performed in the same buffer containing 1.0% (w/v)

CMC-Na for 30 min. The amount of reducing sugars released was determined with the 3,5-dinitrosalicylic acid (DNS) reagent, using xylose or glucose as standard. After incubation, DNS reagent was added and the samples were heated in a boiling water bath for 5 min followed by cooling on ice. The absorbance was then measured at 540 nm. Each assay was performed in triplicate. One unit of xylanase activity is defined as the amount of enzyme required to release one μmole of xylose/glucose reducing-sugar equivalents per minute at 65 °C and pH 7.2. For *p*NPX and *p*NPG, the assay was performed with a final concentration of 0.2 mM at 65 °C for 30 min and the absorbance was measured at 405 nm. One unit of xylanase activity is defined as the amount of enzyme required to release one μmole of *p*-nitrophenol per minute at 65 °C and pH 7.2.

The effect of temperature on enzyme activities was determined by assaying the enzymes at temperatures from 40 to 85 °C using 1% (w/v) beech wood xylan as substrate. Thermal stability of xylanase was assessed by incubated enzyme solutions (0.2 mg/ml) for 4 h at 60 °C, 65 °C, 70 °C and 75 °C, respectively. The relative activities of heat-treated CbXyn10B were measured at definite time intervals.

The effects of pH on enzyme activity were determined at 60 °C under pH ranging from 4 to 11 using 1% (w/v) beech wood xylan as substrate. The reaction buffer contained 30 mM each of 4-(2-hydroxyethyl)-1-piperazineethanesulfonic acid (HEPES), 3-[[1,3-dihydroxy-2-(hydroxymethyl)propan-2-yl]amino]propane-1-sulfonic acid (TAPS), 3-(Cyclohexylamino)-1-propanesulfonic acid (CAPS), 2-(N-morpholino)ethanesulfonic acid (MES) and acetic acid [20], and was adjusted to the appropriate pH with 1 M NaOH. To exclude the possibility of thermo-inactivation at high temperature, the pH stability of the purified enzyme was diluted 100-fold using respective buffers having pH values ranging from 3.0 to 13.0 as described above and were incubated for 4 h at 37 °C [21, 22]. The relative activity of the incubated enzyme was estimated following the procedure described above.

The kinetic parameters were determined by incubating CbXyn10B in 40 mM sodium phosphate buffer (pH 7.2) with birch wood xylan, beech wood xylan and oat spelt xylan at concentrations ranging from 0.2 to 10 mg/ml. All constants were determined at 65 °C to avoid the activity loss during the reaction process. The extent of hydrolysis for each substrate was kept consistent, so that the change of the

inhomogeneous substrate was minimized. Kinetic parameters V_{max}(app) and K_m(app) were acquired by fitting enzymatic activities as a function of substrate concentrations to the Michaelis-Menten equation using non-linear regression of the software Origin 8.0. The k_{cat}(app) was obtained by using the equation k_{cat}(app)=V_{max}(app)/[E], where [E] was the molar concentration of the enzymes.

The effects of metal ions on purified xylanase enzyme activity were determined by incubating the enzyme with a 1, 5 or 10 mM solution of Ca^{2+}, Mg^{2+}, Ni^{2+}, Zn^{2+}, Fe^{3+}, Co^{2+}, Cu^{2+} or EDTA for 1 h at 25 °C. Xylanase activity was measured using 1% (w/v) beech wood xylan as substrate under the standard condition.

2.6. Reaction product analysis

To analyze the hydrolysis mode of xylo-oligosaccharides (XOS), 0.15 mg/ml XOS were incubated with 0.06 μM recombinant xylanase and aliquot samples were collected at different time intervals. For the end products analysis, the reactions were carried out by incubation the XOS and xylans with 12.5 μM CbXyn10B in 40 mM sodium phosphate buffer pH 7.2 at 65 °C for 2 h. All the reactions were terminated by boiling for 5 min. After centrifugation, the soluble products released from the substrates were analyzed using an Agilent 1260 HPLC apparatus (Santa Clara, CA, USA) equipped with a Rezex RPM-monosaccharide column (Phenomenex, CA, USA) and a refractive index detector at a flow rate of 0.3 ml/min water at 75 °C.

2.7. Homology modeling and molecular docking

The 3D structure model of CbXyn10B was generated using the Build Homology Models (MODELER) in Discovery Studio 3.0 (DS 3.0, Accelrys Software Inc., CA, USA). A xylanase from *Paenibacillus barcinonensis* (PbXyn10B, PDB ID 3EMC, 54% identity with CbXyn10B) was selected as the template. The geometry of the loop regions was corrected using Refine Loop/MODELER. The quality of the final model was evaluated by PROCHECK [23] and Profile-3D of DS 3.0.

The molecular docking was performed using AutoDock 4.2 software package [24]. A grid of 60 Å ×50 Å ×50 Å with 0.375 Å spacing was calculated using AutoGrid. Xylopentaose was chosen as the ligand for docking. The results were ranked on the basis of predicted free binding energy. Structural figures were prepared using PyMOL (http://www.pymol.org/).

3. Results

3.1. Sequence analysis of CbXyn10B

CbXyn10B shared the highest sequence identity (96%) with a putative xylanase from *Caldicellulosiruptor kronotskyensis* 2002 (GenBank No. ADQ47206), which is uncharacterized to date. Among characterized xylanases, CbXyn10B shared the highest sequence identity (78%) with XynA from *Caldicellulosiruptor saccharolyticus* (GenBank No. AAA23059), followed by *Pb*Xyn10B from *Paenibacillus barcinonensis* (GenBank No. CAA07174, 54% identity). To further analyze the CbXyn10B sequence, phylogenetic trees generated from 21 xylanase sequences were constructed using the neighbor joining method (Fig. 1). These enzymes are grouped into two subfamilies, intracellular xylanases and extracellular xylanases [25]. CbXyn10B has no signal peptide sequence and possesses two typical conserved motifs of the intracellular xylanases: (AIE_YASL) and (RTDL__PT_EM). Alignment of CbXyn10B and its homologues revealed that Glu139 and Glu247 were putative catalytic residues, and residues along the binding cleft were also highly conserved (Fig. 2).

3.2. Overexpression and purification of CbXyn10B

Recombinant CbXyn10B was abundantly expressed in *E. coli*. As much as 500 mg protein can be obtained from 1 L shaking flask cell culture. The recombinant protein was approximately 40 kDa on a 15% SDS-PAGE gel, in agreement with calculated molecular mass (40.2 kDa) of CbXyn10B (Fig. 3). After heat treatment of the cell lysate at 60 ℃ for 30 min, most of the native *E.coli* protein was denatured and the target protein was purified to approximately 80% purity. Such a simple purification procedure would reduce the overall costs for industrial applications.

3.3. Biochemical characterization of CbXyn10B xylanase

The optimal temperature of CbXyn10B activity was 70 ℃ (Fig. 4a), with >60% of maximum activity retained at 60-75 °C. CbXyn10B had a half-life of about 7.7 h and 3h at 60 ℃ and 65 °C, respectively (Fig. 4b). It showed a half-life of about 30

min at 70 °C, which was obviously lower than the previous reported data (longer than 24 h) [16]. As it is known that thermostability of a protein may be affected by its concentration [26-29], we might use lower protein concentration (0.2 mg/ml) than that of the previous research, which was not clearly reported [16]. At 75 °C, CbXyn10B lost more than 90% of its activity after 5 min.

The optimal pH of CbXyn10B activity was 7.2 (Fig. 4c), with more than 50% of maximum activity retained at pH 6.0-8.0. It also showed high pH stability: more than 85% of the maximum activity retained after incubation at pH values from 4.0 to 12.0 for 4 h (Fig. 4d).

CbXyn10B showed high activity towards various xylan substrates (Table 1). The maximum activity (497 U/mg, 100%) was observed for beech wood xylan, followed by oat spelt xylan (482 U/mg, 96.9%) and birch wood xylan (448 U/mg, 90.1%). CbXyn10B showed similar apparent kinetic parameters for beech wood xylan, oat spelt xylan and birch wood xylan, with K_m(app) values of 1.90 mg/ml, 1.94 mg/ml and 2.16 mg/ml, respectively. In contrast, CbXyn10B exhibited very low activity towards *p*NPX (0.002 U/mg, 0.0004% relative to xylan) and CMC-Na (0.05 U/mg, 0.01% relative to xylan), revealing its high specificity for xylan.

Addition of 5 mM Mg^{2+}, Ca^{2+}, Co^{2+}, Ni^{2+}, Cu^{2+} or Mn^{2+} had no obvious effect on the activity of CbXyn10B (Table 2). However, 1 mM of Zn^{2+} and Fe^{3+} inhibited 20-40% enzymatic activity of CbXyn10B, and the effects were dramatic enhanced (69-100% inhibition) when the concentration of the cations increased to 10 mM. CbXyn10B displayed almost full enzyme activity in the presence of 10 mM EDTA, indicating that cation is not necessary for the catalysis.

3.4. CbXyn10B mode of action

To gain an insight into the mode of enzyme action, xylo-oligosaccharides (XOS) with increasing degrees of polymerization (DP) were hydrolyzed by CbXyn10B, and the released products were analyzed by HPLC at different time intervals (Fig. 5). CbXyn10B showed low activity towards xylotriose (X3) (Fig. 5a). Nevertheless, X3 could be slowly converted into X2 and X1 with excess of enzyme in 2h (Fig. 6a). The hydrolysis rate was obviously enhanced as the substrate DP increased. The hydrolysis of xylotetraose (X4) was much faster with respect to X3, as 45% of X4 was hydrolyzed in 4 min (Fig. 7a). For xylopentaose (X5), the hydrolysis rate was even

faster than X4, with about 80% of X5 hydrolyzed in 4 min. CbXyn10B hydrolyzed xylohexaose (X6) at a similar rate to that of X5.

Analysis of the reaction products profile provides detailed information for the hydrolytic patterns of different XOS substrates. CbXyn10B showed no activity towards xylobiose (X2), even with excess of enzyme (12.5 μM, 0.5 mg/ml) (Fig. 6a). X3 could be completely hydrolyzed into X2 and X1 under the same reaction conditions. Thus, X3 was the smallest substrate for CbXyn10B. For X4, the released product was primary in the form of X2 with a slight amount of X3 (Fig. 5b). CbXyn10B showed preferential action mode on X5 that the released product was predominantly X2 and X3 (Fig. 5c). The accumulated products released from X6 hydrolysis was X3, and to a lesser extent of X2 and X4 (Fig. 5d).

The ultimate hydrolytic products of all the XOS were similar to that for natural xylans (Fig. 6). CbXyn10B could efficiently hydrolyze beech wood xylan, oat spelt xylan and birch wood xylan (Fig. 6b) into X2 and a small amount of X1. This feature makes CbXyn10B to be useful in the enzymatic production of X2.

3.5. Homology modeling and molecular docking

To investigate the structural basis for the action mode of CbXyn10B, we performed a homology modeling and molecular docking study. The overall structure model of CbXyn10B displayed a typical $(\alpha/\beta)_8$-barrel fold (Fig. 8a) [30]. The substrate-binding cleft of CbXyn10B was located on the surface of the protein and consisted of five subsites. The X5 ligand was well docked into the binding cleft (Fig. 8b). Conventionally, the substrate binding subsites are labeled from –3 to +2, with -n at the non-reducing end and +n at the reducing end, while the cleavage occurs between -1 and +1 subsites [8]. At the non-reducing end, the xylose residue at –3 subsite had no obvious interaction with the protein. The xylose residue at the –2 subsite formed hydrogen bonds with side chains of Glu50, Asn51 and Trp297 (Fig. 8c). And the xylose moiety at the –1 subsite formed hydrogen bonds with side chains of Lys54, His87, Asn138, Glu139, Gln215 and Glu247. On the other hand, the xylose residues at the non-reducing end mainly stacked against aromatic residues: the xylose moieties at +1 and +2 subsites interacted with Tyr184 and Phe255, respectively.

4. Discussion

In this study, CbXyn10B was found to be a highly stable xylanase. Compared with its close homologues, it exhibited very high catalytic activity for xylans and showed high substrate specificity (Table 3). The catalytic activities of CbXyn10B towards beech wood xylan and birch wood xylan were approximately 8- to 11-fold higher than iXylC from *C. laeviribosi* HY-21 [31] and 2-fold higher than PbXyn10B from *P. barcinonensis* BP-23 [25]. The catalytic activity of CbXyn10B towards oat spelt xylan was approximately 74-fold higher than XynA from *C. saccharolyticus* [32], and was 5.5- to 8-fold higher than iXylC and XynBE18 from *Paenibacillus* sp., respectively [33]. Interestingly, CbXyn10B showed extremely low activity (about 0.002 U/mg) toward *p*NP-xylopyranoside (*p*NPX), which was approximately 143-fold and 28,900-fold lower than that of PbXyn10B and iXylC, respectively. In addition, the specific activity of CMC-Na was only 0.05 U/mg, which was 240-fold lower than that of TmxB from *Thermotoga maritima* MSB8 [34].

Unlike some xylanases [35, 36], CbXyn10B was insensitive to a variety of divalent ions (Table 2). EDTA also did not affect CbXyn10B activity, suggesting that no metal is essential for this enzyme. This is also different from some xylanases that require Mg^{2+} and Ca^{2+}. For example, addition of $MgCl_2$ to a GH10 xylanase from *Bacillus* sp. NG-27 (BSX; PDB code 2F8Q) greatly enhanced its activity [37]. A Ca^{2+} ion was found in the *Pseudomonas fluorescens* sp. xylanase (PFX; PDB code 1CLX) to protect it from proteinase inactivation and thermal unfolding [38].

As commonly observed in GH10 xylanases, the catalytic efficiency of CbXyn10B was improved with increasing the polymerization degree of XOS. The activities towards various XOS had the following order: X6=X5>X4>X3>>X2, implying there might be five xylose-binding subsites in CbXyn10B active site (Fig. 8b).

The hydrolytic pattern analysis allows a more detailed understanding of the substrate recognition mechanism. CbXyn10B was completely ineffective on X2 substrate, which implied that X2 nonproductively bound at the -2 and -1 subsite instead of the productive -1 and +1 subsites. This is consistent with our docking result that xylose moieties formed much stronger interactions with the residues at the -2 and

-1 subsites compared with other subsites (Fig. 8c). CbXyn10B exhibited low activity towards X3, suggesting that only a small number of X3 molecules could form productive complex. It is possible most X3 molecules may be trapped in the region from –3 and –1 subsites and form a nonproductive complex (Fig. 7b).

X4 was cleaved primarily into X2, indicating X4 preferred to bind from -2 to +2 subsites of CbXyn10B. Meanwhile, a small amount of X1 and X3 also formed, suggesting a minor amount of X4 also bound at -3 to +1 subsites. Molecular docking result revealed that the xylose residue at +2 subsite stacked against the phenyl group of Phe255 and formed hydrogen bonds with side chain of Asn185. In contrast, no obvious interaction was observed at –3 subsite. The tightly binding of subsite +2 over -3 may explain why the binding at -2 to +2 subsites was favored.

X5 had preferential mode of cleavage that released X2 and X3, suggesting a predominant binding position from -3 to +2 subsites (Fig. 7b). This was consistent with the molecular docking result that the carbohydrate chain of X5 lined well in the binding cleft of CbXyn10B. The docked complex didn't show any direct xylose-enzyme interaction at -3 subsite. However, the faster hydrolysis rate of X5 compared to X4 suggested a catalytically important role of this subsite. We speculated that residues at the -3 subsite possibly indirectly interact with xylose moiety via water molecules. This kind of water-mediated interaction was found in a xylanase from *G. stearothermophilus* T-6 [39].

The majority of accumulated product for X6 hydrolysis was X3. This reveals that the major binding mode of the substrate is from -3 to +2 subsites with a free xylose moiety at the reducing end (Fig. 7b). Meanwhile, a smaller amount of X2 and X4 also formed, suggesting a minor binding mode that with a free xylose moiety at the non-reducing end.

CbXyn10B can efficiently hydrolyze various xylans into X2, which has been proven to have potential to improve health by maintaining a balanced intestinal microflora [40]. The enzymatic production of X2 is highly advantageous compared with chemical methods because of energy conservation, environment-friendly and less byproducts [41, 42]. Moreover, CbXyn10B functions efficiently at elevated temperatures, which in turn reduces the risk of microbial contamination, improves reaction rates, and increases substrate solubility, which highlights its potential in the

large-scale production of X2.

5. Conclusion

In this study, *xyn10B* gene from *C. bescii* sp. nov. DSM 6725 was overexpressed in *E. coli* and systematically characterized. The recombinant xylanase has high activity for xylans and high substrate specificity. It shows high thermostability and a wide range of pH stability. No metal ion is required for its catalysis and thermostability. The enzyme hydrolyzes various xylans into xylobiose, which highlights its potential in the large-scale production of xylobiose. The action mode of the enzyme was studied by product analysis, homology modeling and molecular docking, which provide an insight into the structural basis for its substrate recognition.

Abbreviations

*p*NPX: p-nitrophenyl-β-D-xylopyranoside; GH: glycoside hydrolase; CMC-Na: Sodium carboxymethyl cellulose; XOS: xylo-oligosaccharides; X1-X6: xylose, xylobiose, xylotriose, xylotetraose, xylopentaose and xylohexaose.

Acknowledgements

This work was supported by the National High Technology Research and Development Program of China (863 Program), the National Basic Research Program of China (973 Program), Natural Science Foundation of China (31470788), and Research Fund for the Doctoral Program of Higher Education of China (No. 20110073120062).

References

[1] R.A. Prade, Biotech. Genet. Eng. Rev. 13 (1995) 100-131.

[2] R. Chávez, P. Bull, J. Eyzaguirre, J. Biotechnol. 123 (2006) 413-433.

[3] S. Ahmed, S. Riaz, A. Jamil, Appl. Microbiol. Biotechnol. 84 (2009) 19-35.

[4] D. Shallom, Y. Shoham, Curr. Opin. Microbiol. 6 (2003) 219-228.

[5] K.K. Wong, L.U. Tan, J.N. Saddler, Microbiol. Rev. 52 (1988) 305-317.

[6] C.S. Rye, S.G. Withers, Curr. Opin. Chem. Biol. 4 (2000) 573-580.

[7] T. Collins, C. Gerday, G. Feller, FEMS Microbiol. Rev. 29 (2005) 3-23.

[8] A. Pollet, J.A. Delcour, C.M. Courtin, Crit. Rev. Biotechnol. 30 (2010) 176-191.

[9] S.R. Andrews, S.J. Charnock, J.H. Lakey, G.J. Davies, M. Claeyssens, W. Nerinckx, M. Underwood, M.L. Sinnott, R.A. Warren, H.J. Gilbert, J. Biol. Chem. 275 (2000) 23027-23033.

[10] V. Ducros, S.J. Charnock, U. Derewenda, Z.S. Derewenda, Z. Dauter, C. Dupont, F. Shareck, R. Morosoli, D. Kluepfel, G.J. Davies, J. Biol. Chem. 275 (2000) 23020-23026.

[11] Q.K. Beg, M. Kapoor, L. Mahajan, G.S. Hoondal, Appl. Microbiol. Biotechnol. 56 (2001) 326-338.

[12] S. Subramaniyan, P. Prema, Crit. Rev. Biotechnol. 22 (2002) 33-64.

[13] D. Verma, T. Satyanarayana, Bioresour. Technol. 117 (2012) 360-367.

[14] S.J. Yang, I. Kataeva, S.D. Hamilton-Brehm, N.L. Engle, T.J. Tschaplinski, C. Doeppke, M. Davis, J. Westpheling, M.W. Adams, Appl. Environ. Microbiol. 75 (2009) 4762-4769.

[15] I.A. Kataeva, S.J. Yang, P. Dam, F.L. Poole II, Y. Yin, F. Zhou, W.C. Chou, Y. Xu, L. Goodwin, D.R. Sims, J.C. Detter, L.J. Hauser, J. Westpheling, M.W. Adams, J. Bacteriol. 191 (2009) 3760-3761.

[16] X. Su, Y. Han, D. Dodd, Y.H. Moon, S. Yoshida, R.I. Mackie, I.K. Cann, Appl. Environ. Microbiol. 79 (2013) 1481-1490.

[17] S.F. Altschul, T.L. Madden, A.A. Schäffer, J. Zhang, Z. Zhang, W. Miller, D.J. Lipman, Nucleic Acids Res. 25 (1997) 3389-3402.

[18] K. Tamura, D. Peterson, N. Peterson, G. Stecher, M. Nei, S. Kumar, Mol. Biol. Evol. 28 (2011) 2731-2739.

[19] M.A. Larkin, G. Blackshields, N.P. Brown, R. Chenna, P.A. McGettigan, H. McWilliam, F. Valentin, I.M. Wallace, A. Wilm, R Lopez, J.D. Thompson, T.J. Gibson, D.G. Higgins, Bioinformatics 23 (2007) 2947-2948.

[20] T. Juhász, Z. Szeltner, L. Polgár, FEBS Lett. 580 (2006) 3493-3497.

[21] K. Ratanakhanokchai, K.L. Kyu, M. Tanticharoen, Appl. Environ. Microbiol. 65 (1999) 694-697.

[22] S. Wu, B. Liu, X. Zhang, Appl. Microbiol. Biotechnol. 72 (2006) 1210-1216.

[23] R.A. Laskowski, M.W. MacArthur, D.S. Moss, J.M. Thornton, J. Appl. Crystallogr. 26 (1993) 283-291.

[24] G.M. Morris, D.S. Goodsell, R.S. Halliday, R. Huey, W.E. Hart, R.K. Belew, A.J. Olson, J. Comput. Chem. 19 (1998) 1639-1662.

[25] O. Gallardo, P. Diaz, F.I. Pastor, Appl. Microbiol. Biotechnol. 61 (2003) 226-233.

[26] S. Iametti, S. Cairoli, B. De Gregori, F. Bonomi, J. Agric. Food Chem. 43 (1995) 53-58.

[27] V. Consalvi, R. Chiaraluce, L. Politi, A. Pasquo, M. De Rosa, R. Scandurra, Biochim. Biophys. Acta. 1202 (1993) 207-215.

[28] B.I. Kurganov, B.A. Kornilaev, N.A. Chebotareva, V.P. Malikov, V.N. Orlov, A.E. Lyubarev, N.B. Livanova, Biochemistry 39 (2000) 13144-13152.

[29] M.L. Galisteo, P.L. Mateo, J.M. Sanchez-Ruiz, Biochemistry 30 (1991) 2061-2066.

[30] G. Davies, B. Henrissat, Structure 3 (1995) 853-859.

[31] Y. Kim do, M.K. Han, H.W. Oh, K.S. Bae, T.S. Jeong, S.U. Kim, D.H. Shin, I.H. Kim, Y.H. Rhee, K.H. Son, H.Y. Park, Bioresour. Technol. 101 (2010) 8814-8821.

[32] E. Lüthi, N.B. Jasmat, P.L. Bergquist, Appl. Environ. Microbiol. 56 (1990) 2677-2683.

[33] P. Shi, J. Tian, T. Yuan, X. Liu, H. Huang, Y. Bai, P. Yang, X. Chen, N. Wu, B. Yao, Appl. Environ. Microbiol. 76 (2010) 3620-3624.

[34] Z.Q. Jiang, W. Denga, Y.P. Zhua, L.T. Li, Y.J. Sheng, K. Hayashi, Journal of Molecular Catalysis B: Enzymatic 27 (2003) 207-213.

[35] S. Wu, B. Liu, X. Zhang, Appl. Microbiol. Biotechnol. 72 (2006) 1210-1216.

[36] A. Khasin, I. Alchanati, Y. Shoham, Appl. Environ. Microbiol. 59 (1993) 1725-1730.

[37] K. Manikandan, A. Bhardwaj, N. Gupta, N.K. Lokanath, A. Ghosh, V.S. Reddy, S. Ramakumar, Protein Sci. 15 (2006) 1951-1960.

[38] T.D. Spurway, C. Morland, A. Cooper, I. Sumner, G.P. Hazlewood, A.G. O'Donnell, R.W. Pickersgill, H.J. Gilbert, J. Biol. Chem. 272 (1997) 17523-17530.

[39] G. Zolotnitsky, U. Cogan, N. Adir, V. Solomon, G. Shoham, Y. Shoham, Proc. Natl. Acad. Sci. U S A 101 (2004) 11275-11280.

[40] A.A. Aachary, S.G. Prapulla, Comprehensive Reviews in Food Science and Food Safety 10 (2011) 2-16.

[41] D. Chapla, P. Pandit, A. Shah, Bioresour. Technol. 115 (2012) 215-221.

[42] H. Yang, K. Wang, X. Song, F. Xu, Bioresour. Technol. 102 (2011) 7171-7176.

Figure captions

Fig. 1. Neighbor-Joining tree of 21 xylanases sequences. Numbers on nodes correspond to percentage bootstrap values for 1000 replicates.

Fig. 2. Multiple sequence alignment of CbXyn10B with its homologues. The two catalytic glutamate residues of CbXyn10B are marked with black asterisks. The residues along the binding cleft are marked by arrows. The motifs a (AIE_YASL) and b (RTDL__PT_EM) of signal peptide-less xylanases are highlighted. *C. bescii* DSM 6725: GenBank No. ACM59337; *C. Saccharolyticus*: GenBank No. AAA23059; *P. barcinonensis* BP-23: GenBank No. CAA07174; *Paenibacillus* sp. E18: GenBank No. ACY69972; *C. laeviribosi* HY-21: GenBank No. ADE08352; *Alicyclobacillus* sp. A4: GenBank No. ACY69980; *B. halodurans* S7: GenBank No. Q17TM8; *Bacillus* sp. NG-27: GenBank No. AAB70918.

Fig. 3. SDS-PAGE analysis of purified recombinant CbXyn10B. Lane M protein marker; Lane 1 supernatant of crude enzyme incubated at 60 °C for 30 min; Lane 2 CbXyn10B purified by Ni-NTA affinity chromatography.

Fig. 4. Enzymatic properties of recombinant CbXyn10B. (a) Temperature effect on CbXyn10B activity; (b) pH effect on CbXyn10B activity at defined pH ranging from 4 to 11; (c) Thermal stability of CbXyn10B at 60 °C, 65 °C and 70 °C; (d) pH stability of CbXyn10B.

Fig. 5. HPLC analysis of hydrolytic products released from X3 (a), X4 (b), X5(c), and X6 (d). Reactions (300 µl) containing 0.15 mg/ml substrate were incubated at 65 °C in 40 mM sodium phosphate buffer pH 7.2 with 0.06 µM CbXyn10B for the indicated

times.

Fig. 6. HPLC analysis of the ultimate products released from XOS (a) and xylan (b) hydrolysis by 12.5 μM CbXyn10B at 65 °C in 40 mM sodium phosphate buffer (pH 7.2) for 2 h.

Fig. 7. Activity of CbXyn10B against XOS and the mode action of enzyme. (a) XOS (X3-X6) consumption during the reaction process. The initial amount of XOS was taken as 100%. (b) Suggested binding form of XOS in the enzyme-substrate complexes. XOS shown are: X3 (■), X4 (●), X5 (▲), and X6 (◆).

Fig. 8. Molecular modeling and substrate docking of CbXyn10B with X5. (a) The overall structure of the modeled CbXyn10B. The putative catalytic residues are shown as sticks. (b) Solvent-accessible surface representing the substrate-binding cleft of CbXyn10B. The binding subsites (–3 to +2) are labelled and the substrate X5 is shown by stick and ball. (c) The CbXyn10B-X5 complex structure. The hydrogen bonding network was shown in dashed line.

Table 1 Substrate specificity of recombinant CbXyn10B

Substrate	Specific activity (IU mg^{-1})[a]	K_m(app)[f] (mg ml^{-1})	k_{cat}(app)[f] (s^{-1})	k_{cat}/K_m(app)[f] (ml mg^{-1} s^{-1})
Beech wood xylan	497[b]	1.90	378.4	199.2
Oat spelt xylan	482[b]	1.94	355.8	183.4
Birch wood xylan	448[b]	2.16	321.6	148.8
CMC-Na (low viscosity)	0.05[c]	ND[g]	ND	ND
*p*NPX	0.002[d]	ND	ND	ND
*p*NPG	-[e]	ND	ND	ND

[a] One international unit of enzyme activity was defined as the amount of enzyme required to release 1 μmol reducing sugar (for xylans and CMC-Na) or *p*-nitrophenol (for *p*NPX and *p*NPG) min^{-1} under standard assay conditions.
[b] The data were obtained using 0.03 μM CbXyn10B with 1% xylan for 5 min at 65 °C and pH 7.2.
[c] The data were obtained using 12.5 μM CbXyn10B with 1% CMC for 30 min at 65 °C and pH 7.2.
[d] The data were obtained using 12.5 μM CbXyn10B with 0.2 mM *p*NPX for 30 min at 65 °C and pH 7.2.
[e] Not detectable.
[f] The (app) designations are used because the inhomogeneous substrates changes during the reaction, so the actual value observed depends upon the source and batch of xylan used, as well as the extent of reaction followed. These parameters were kept consistent in all studies described here.
[g] Not detected.

Table 2 Effect of metal ions on CbXyn10B activity

	Relative activity **(%)**		
	1 mM	5 mM	10mM
Control	100.0	100.0	100.0
$MgCl_2$	100±1.9	101±0.7	97±0.6
$CaCl_2$	102±0.9	100±0.3	101±0.9
$CoCl_2$	99±0.3	98±0.4	76±1.8
$NiCl_2$	96±0.7	88±1.0	82±0.3
$CuCl_2$	100±0.9	93±1.8	88±1.5
$MnCl_2$	94±3.0	81±1.5	68±0.6
$ZnCl_2$	88±0.5	52±1.0	31±0.9
$FeCl_3$	65±0.2	41±0.7	0
EDTA	98±1.3	98±2.1	97±1.2

Table 3 Comparison of enzymatic properties and specific activities of CbXyn10B and its homologues

Enzyme	Source	Specific activity (IU mg^{-1})					Optimum temperature (°C)	Optimum pH	References
		Beech wood xylan	Birch wood xylan	Oat spelt xylan	*p*NPX	*p*NPG2			
CbXyn10B	*C. bescii* DSM 6725	497	448	482	2×10^{-3}	-[a]	70-72	7.2	this study
XynA	*C. saccharolyticus*	NA[b]	NA	6.5	NA	NA	70	5.5-6	[32]
PbXyn10B	*P. barcinonensis* BP-23	249×10^{-3}	233×10^{-3}	313×10^{-3}	286×10^{-3}	42×10^{-3}	40	5.5	[25]
XynBE18	*Paenibacillus* sp. E18	NA	61.6	59.6	NA	NA	50	7.5-9	[33]
iXylC	*C. laeviribosi* HY-21	43.6	52.4	88.6	57.8	140.5	50	7.5	[31]
BSX	*Bacillus* sp. NG-27	NA	NA	NA	NA	NA	70	8.4	[37]

[a] Not detected.
[b] Not available.

Highlights

- A xylanase gene (*xyn10B*) from the thermophilic bacterium *Caldicellulosiruptor bescii* was cloned, overexpressed and the recombinant enzyme CbXyn10B was systematically charaterized.
- CbXyn10B exhibited high xylanase activity and thermo-/pH stability.
- CbXyn10B displayed high substrate specificity and released high levels of physiologically important xylooligosaccharides from xylans.

***Graphical Abstract (for review)**

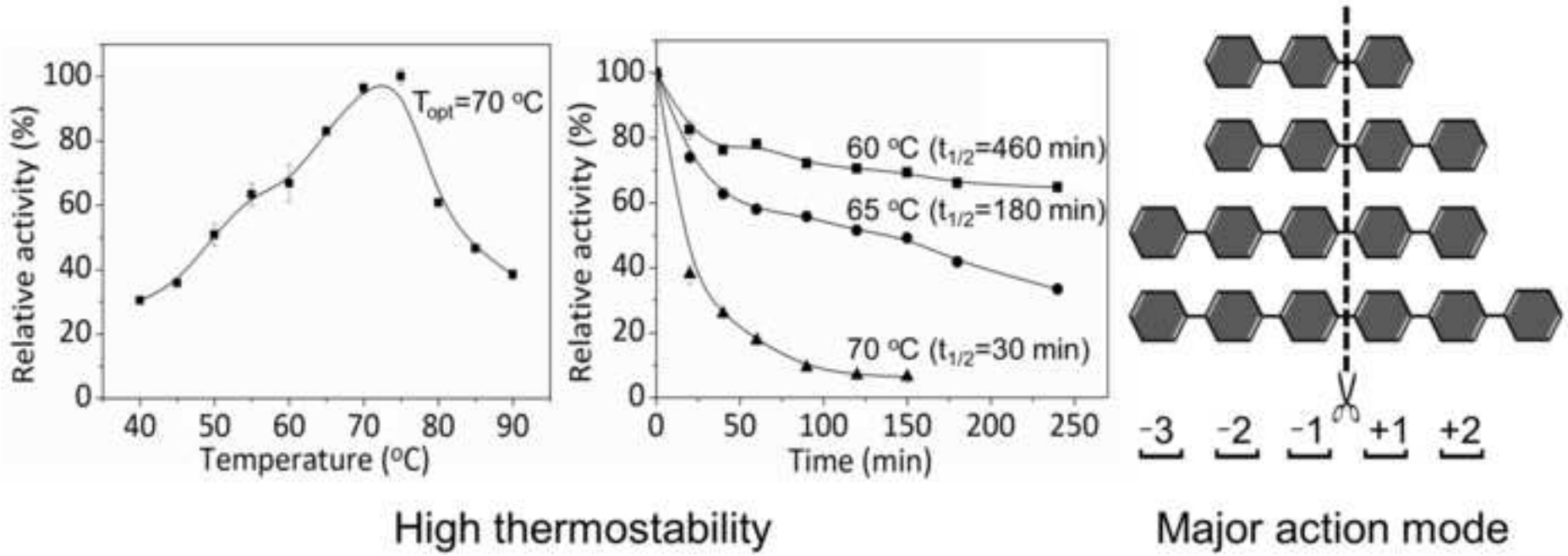

High thermostability

Major action mode

Figure 1

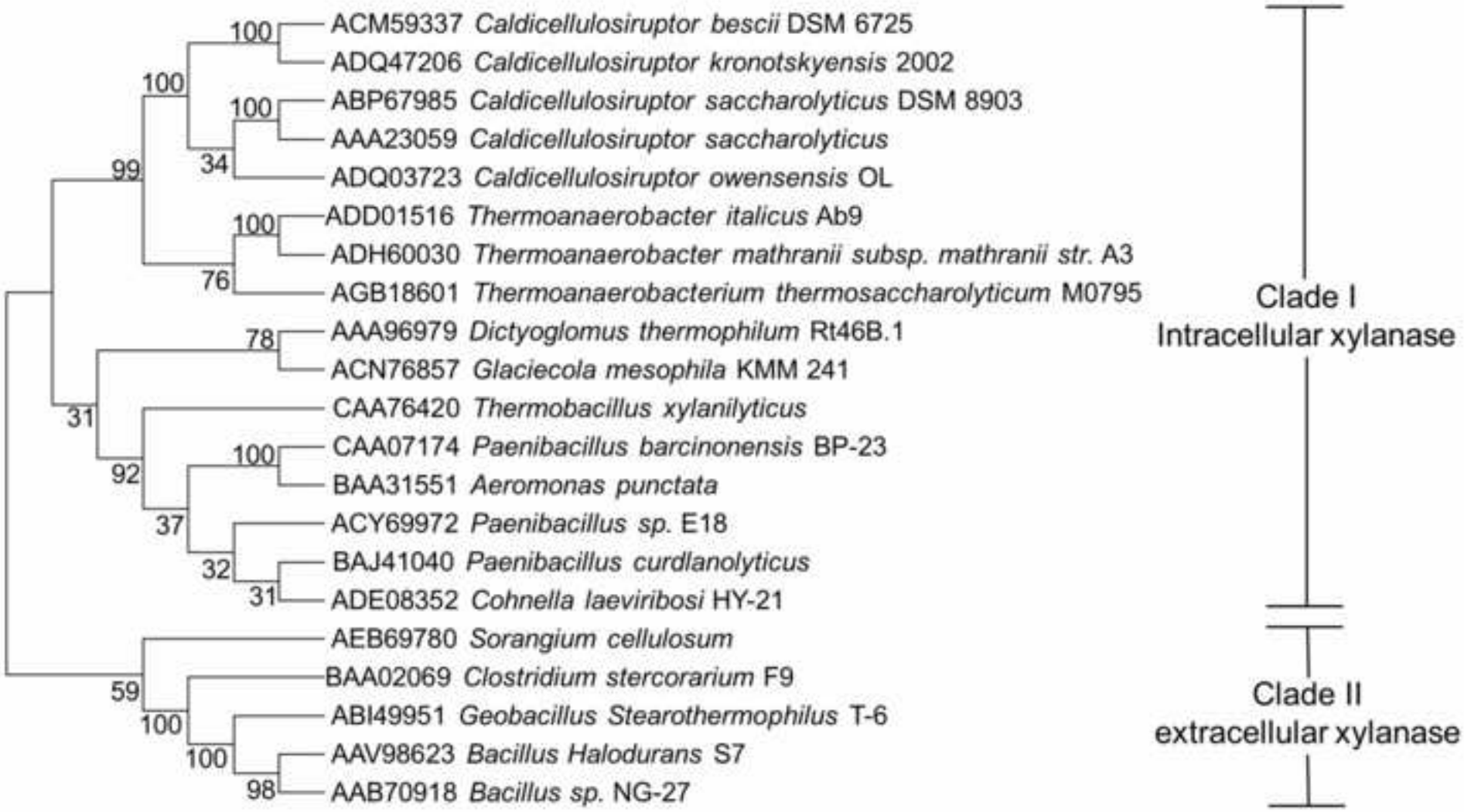
100
100
100
34
99
100
76
78
31
92
100
37
32
31
59
100
100
98
ACM59337 Caldicellulosiruptor bescii DSM 6725
ADQ47206 Caldicellulosiruptor kronotskyensis 2002
ABP67985 Caldicellulosiruptor saccharolyticus DSM 8903
AAA23059 Caldicellulosiruptor saccharolyticus
ADQ03723 Caldicellulosiruptor owensensis OL
ADD01516 Thermoanaerobacter italicus Ab9
ADH60030 Thermoanaerobacter mathranii subsp. mathranii str. A3
AGB18601 Thermoanaerobacterium thermosaccharolyticum M0795
AAA96979 Dictyoglomus thermophilum Rt46B.1
ACN76857 Glaciecola mesophila KMM 241
CAA76420 Thermobacillus xylanilyticus
CAA07174 Paenibacillus barcinonensis BP-23
BAA31551 Aeromonas punctata
ACY69972 Paenibacillus sp. E18
BAJ41040 Paenibacillus curdlanolyticus
ADE08352 Cohnella laeviribosi HY-21
AEB69780 Sorangium cellulosum
BAA02069 Clostridium stercorarium F9
ABI49951 Geobacillus Stearothermophilus T-6
AAV98623 Bacillus Halodurans S7
AAB70918 Bacillus sp. NG-27
Clade I
Intracellular xylanase
Clade II
extracellular xylanase

Figure 2

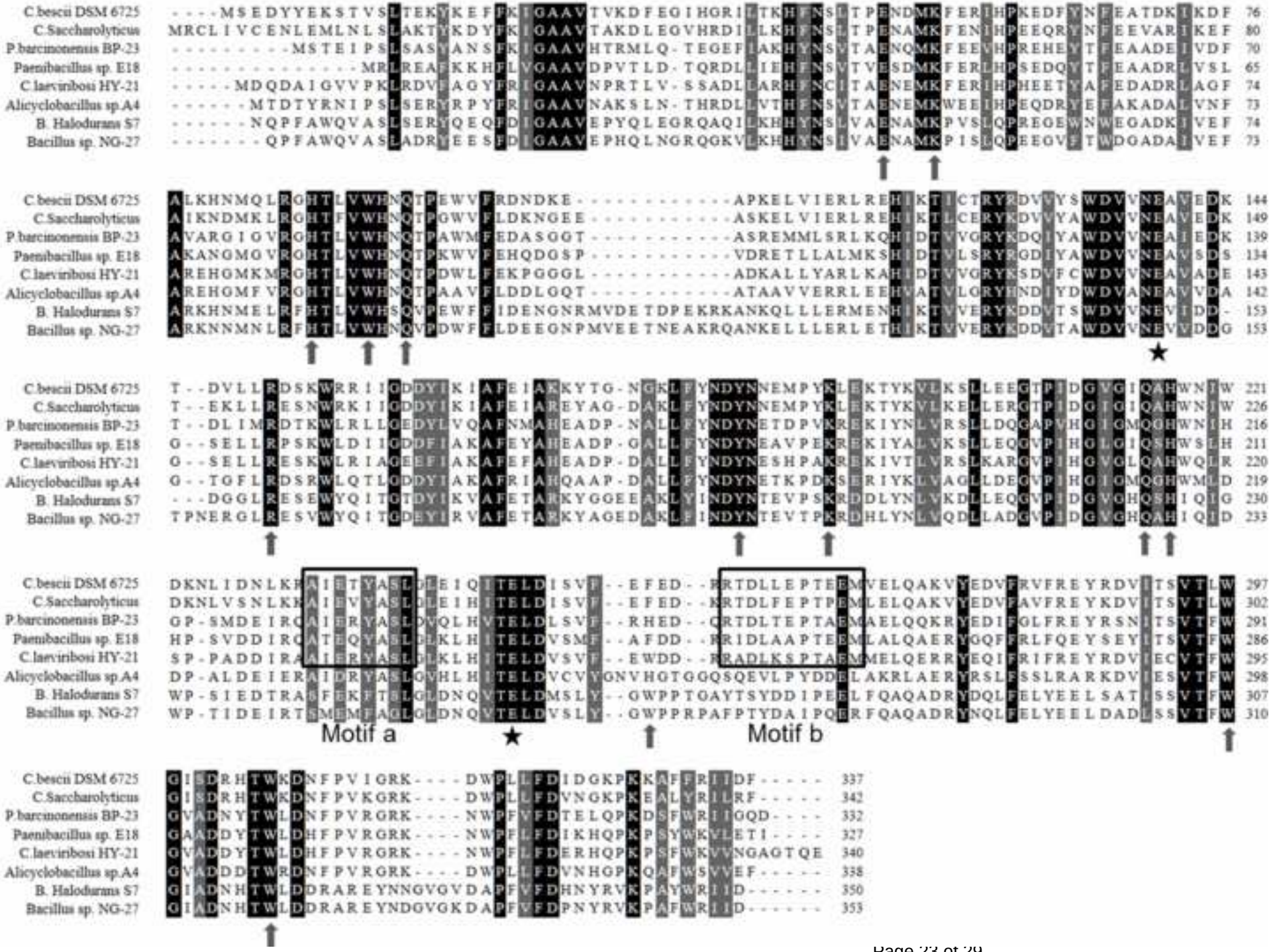
C.bescii DSM 6725
C.Saccharolyticus
P.barcinonensis BP-23
Paenibacillus sp. E18
C.laeviribosi HY-21
Alicyclobacillus sp.A4
B. Halodurans S7
Bacillus sp. NG-27
Motif a
Motif b

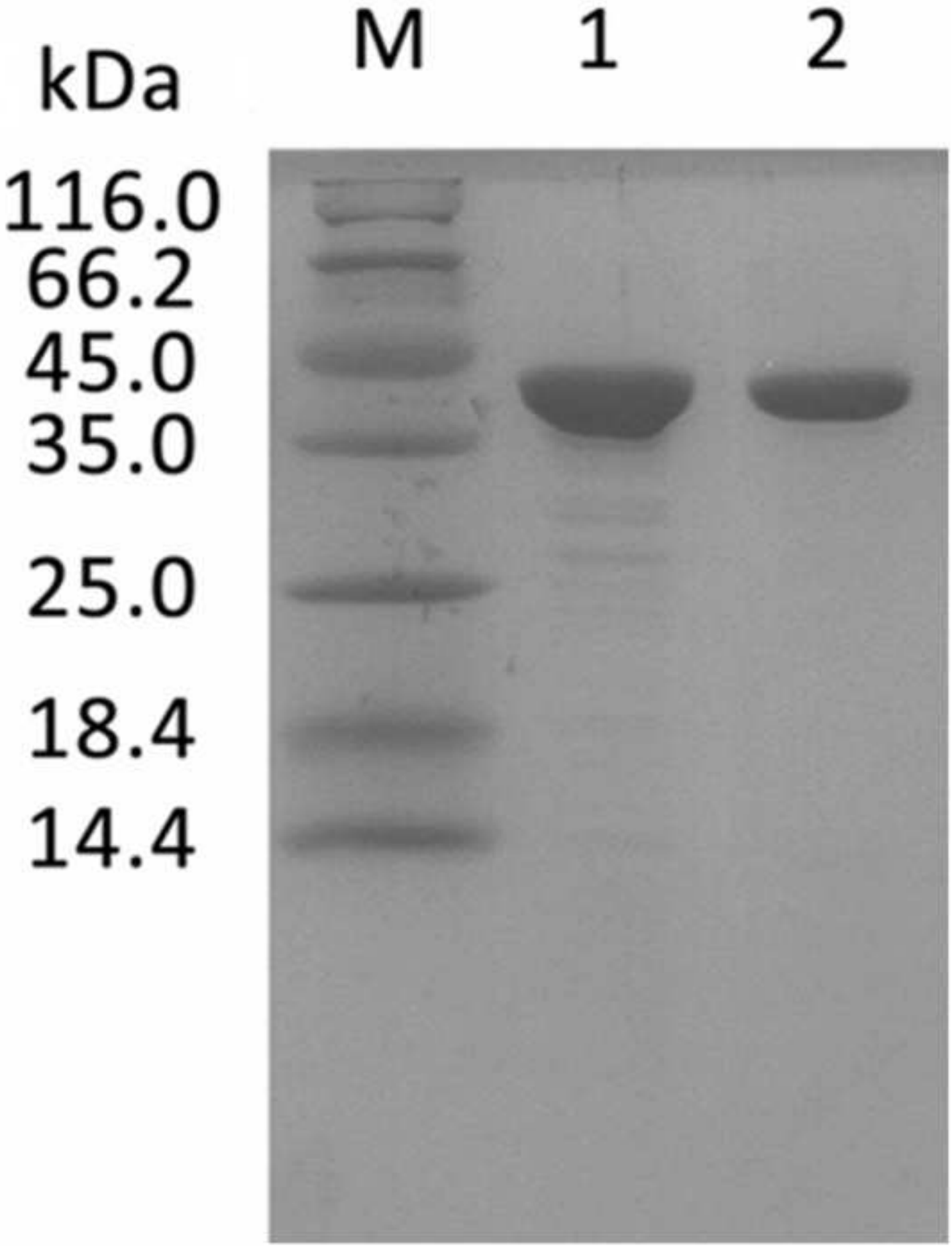

Figure 4

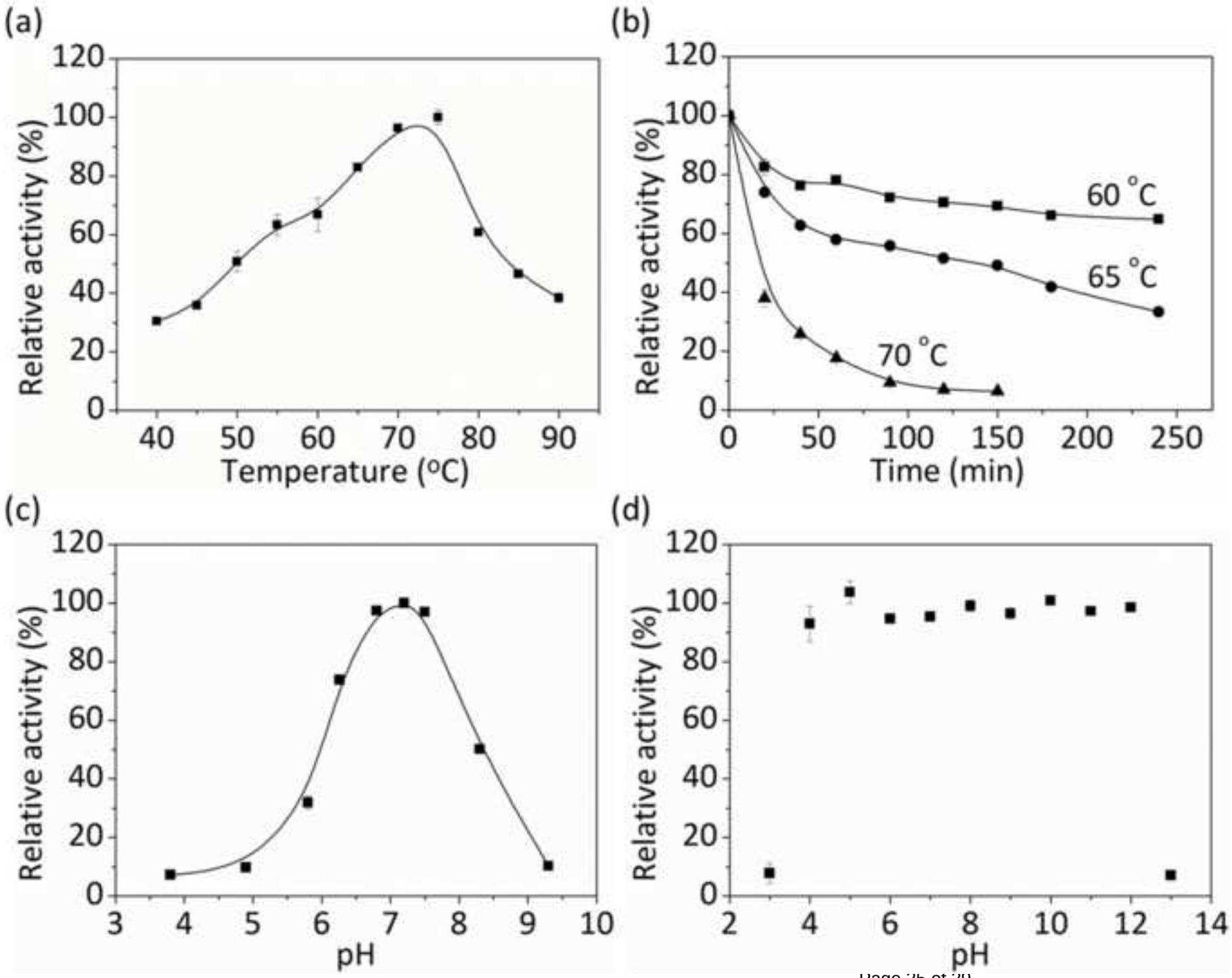
(a)
Relative activity (%)
Temperature (°C)
(b)
Relative activity (%)
Time (min)
60 °C
65 °C
70 °C
(c)
Relative activity (%)
pH
(d)
Relative activity (%)
pH

Figure 5

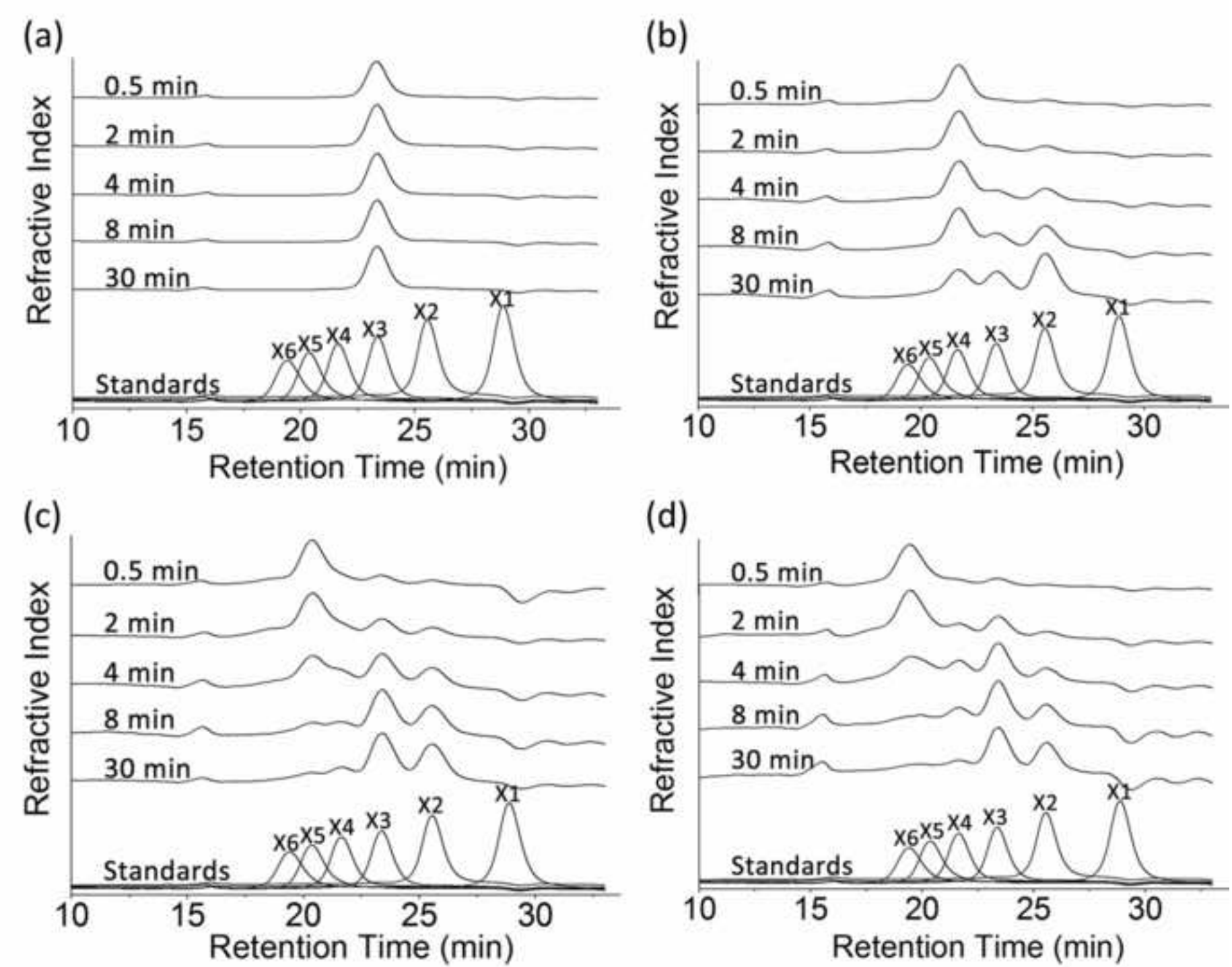
(a)
0.5 min
2 min
4 min
8 min
30 min
Standards
X1
X2
X3
X4
X5
X6
Refractive Index
10
15
20
25
30
Retention Time (min)
(b)
0.5 min
2 min
4 min
8 min
30 min
Standards
X1
X2
X3
X4
X5
X6
Refractive Index
10
15
20
25
30
Retention Time (min)
(c)
0.5 min
2 min
4 min
8 min
30 min
Standards
X1
X2
X3
X4
X5
X6
Refractive Index
10
15
20
25
30
Retention Time (min)
(d)
0.5 min
2 min
4 min
8 min
30 min
Standards
X1
X2
X3
X4
X5
X6
Refractive Index
10
15
20
25
30
Retention Time (min)

Figure 6

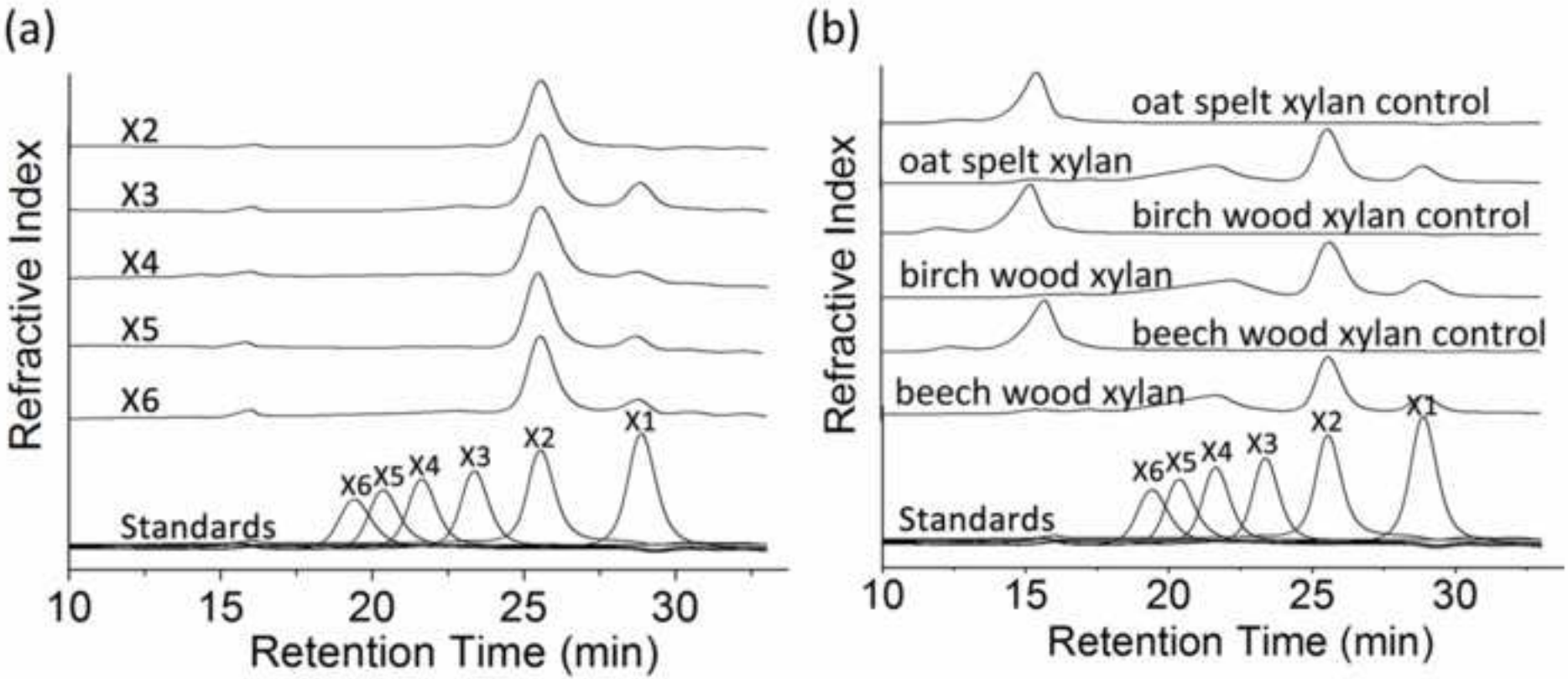
(a)
Refractive Index
X2
X3
X4
X5
X6
X6 X5 X4 X3 X2 X1
Standards
10
15
20
25
30
Retention Time (min)
(b)
Refractive Index
oat spelt xylan control
oat spelt xylan
birch wood xylan control
birch wood xylan
beech wood xylan control
beech wood xylan
X6 X5 X4 X3 X2 X1
Standards
10
15
20
25
30
Retention Time (min)

Figure 7

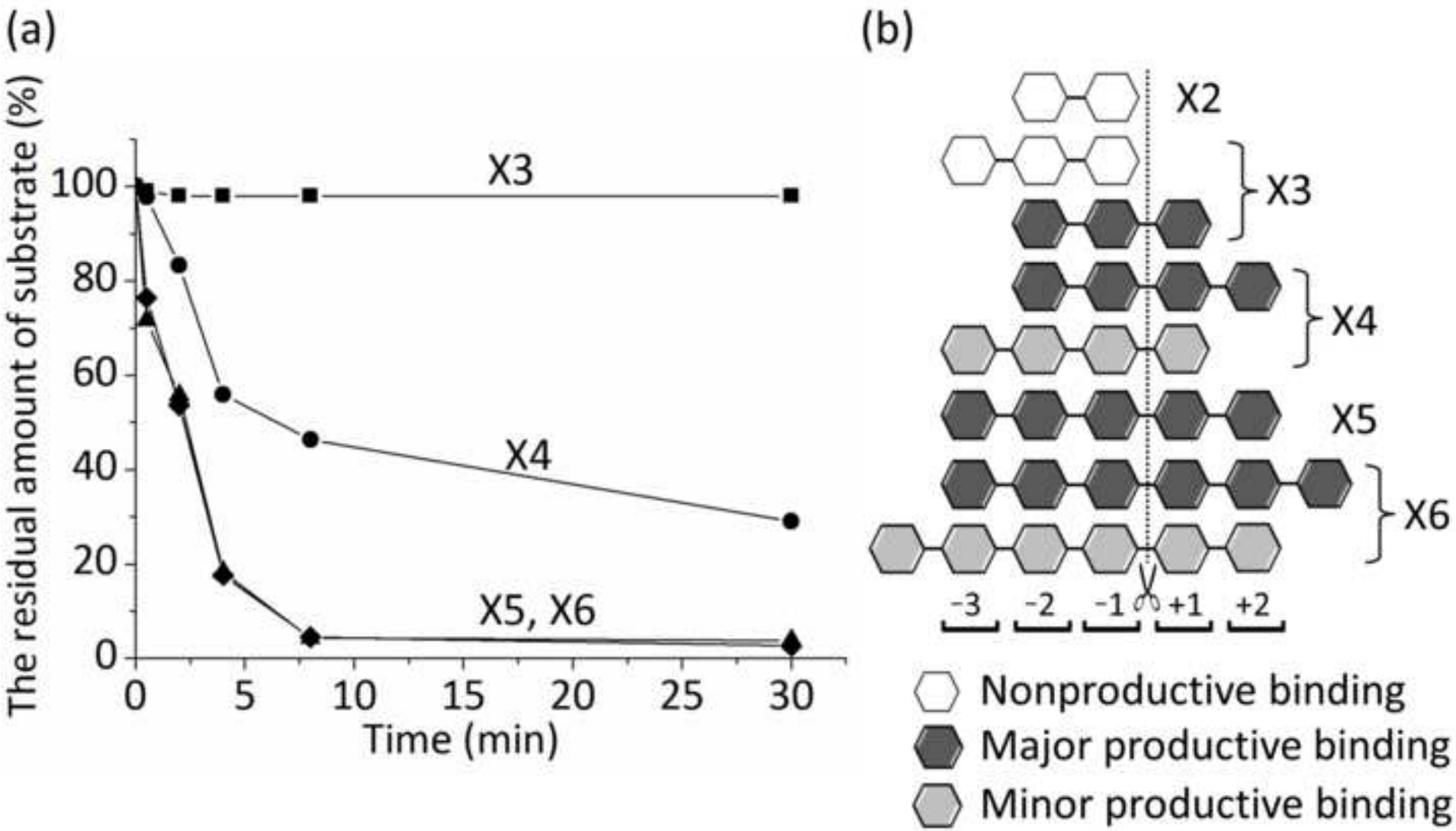
(a)
The residual amount of substrate (%)
100
80
60
40
20
0
0
5
10
15
20
25
30
Time (min)
X3
X4
X5, X6
(b)
X2
X3
X4
X5
X6
-3
-2
-1
+1
+2
Nonproductive binding
Major productive binding
Minor productive binding

Figure 8

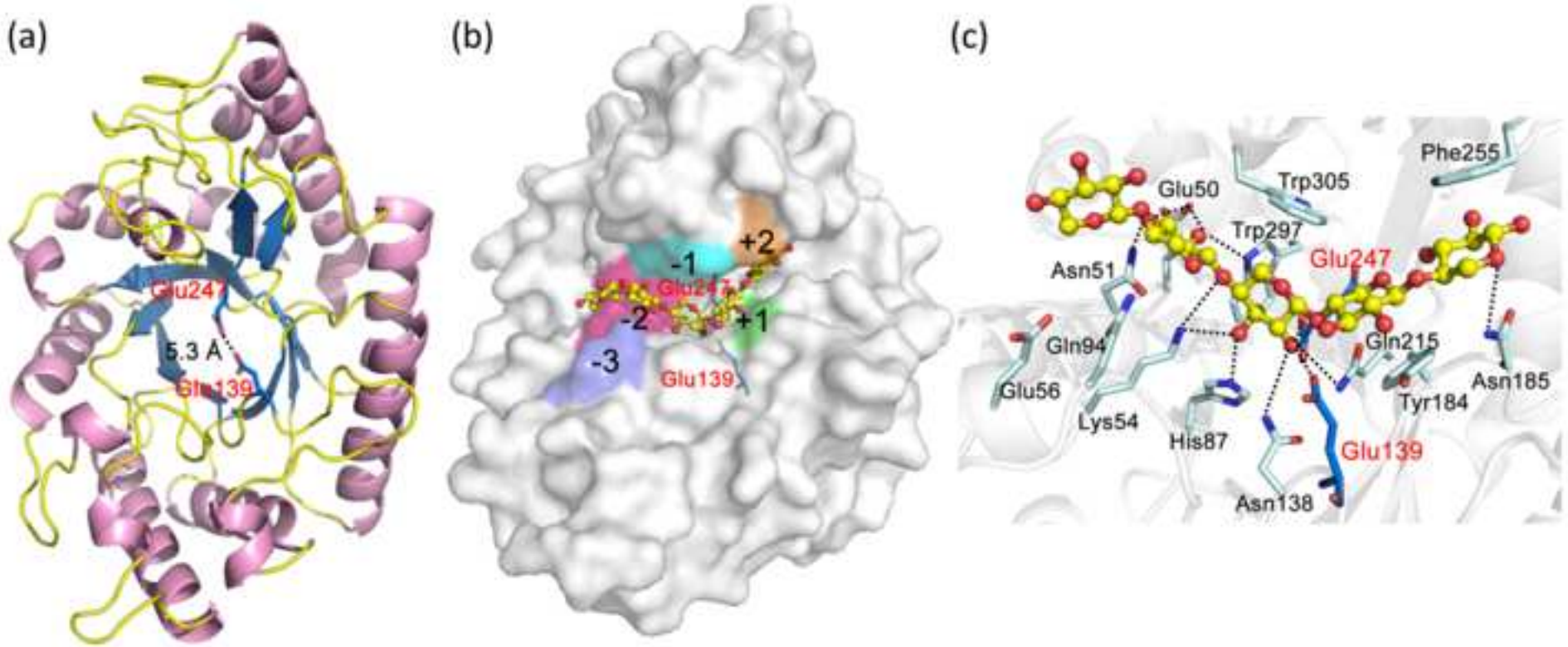
(a)
Glu247
5.3 Å
Glu139
(b)
+2
-1
Glu247
-2
+1
-3
Glu139
(c)
Phe255
Glu50
Trp305
Trp297
Asn51
Glu247
Gln94
Gln215
Asn185
Glu56
Tyr184
Lys54
His87
Glu139
Asn138